Heliyon 5 (2019) e01692

Contents lists available at ScienceDirect

Heliyon

journal homepage: www.heliyon.com

β-Cyclodextrin complex improves the bioavailability and antitumor potential of cirsiliol, a flavone isolated from *Leonotis nepetifolia* (Lamiaceae)

Ana P. Oliveira [a,b], Andressa L.N. Silva [a], Lucas G.F.C. Viana [a], Mariana G. Silva [a,b], Érica M. Lavor [a,b], Raimundo G. Oliveira-Júnior [a], Edilson B. Alencar-Filho [a], Ricardo S. Lima [a], Rosemairy L. Mendes [a], Larissa A. Rolim [a,b], Débora S.C. Anjos [c], Leslie R.M. Ferraz [d], Pedro J. Rolim-Neto [d], Maria F.S. Silva [e], Claudia do Ó. Pessoa [e], Jackson R.G.S. Almeida [a,b,*]

[a] *Center for Studies and Research of Medicinal Plants (NEPLAME), Federal University of San Francisco Valley, Petrolina, Pernambuco, CEP 56.304-917, Brazil*
[b] *Post-Graduate Program in Biotechnology (RENORBIO), Recife, Pernambuco, CEP 52.171-900, Brazil*
[c] *Federal Institute of Science and Technology of Sertão Pernambucano, Petrolina, Pernambuco, CEP 56316-686, Brazil*
[d] *Federal University of Pernambuco, Recife, Pernambuco, CEP 50.670-901, Brazil*
[e] *Federal University of Ceará, Fortaleza, Ceará, CEP 60.020-181, Brazil*

ARTICLE INFO

Keywords:
Pharmaceutical chemistry
Pharmaceutical science
Lamiaceae
Flavone
Inclusion complexes
Antitumor effect

ABSTRACT

Cirsiliol is a flavone found in many Lamiaceae species with high cytotoxic activity against tumor cell lines. Although cirsiliol is being used in cancer therapy, its pharmacological potential is limited by its low solubility and bioavailability. In this paper, a cirsiliol-β-cyclodextrin inclusion complex was developed in order to increase its solubility and bioavailability. The formation of inclusion complex was proved by scanning electron microscopy, Fourier-transform infrared spectroscopy (FTIR) and nuclear magnetic resonance (NMR) and solubility increment was verified through the ultraviolet-visible (UV-Vis) method. The cytotoxic effect against tumor cells (PC3, HCT-116 and HL-60 human cell lines, and S-180 murine cell line) and the antitumor activity in mice bearing sarcoma S-180 were also investigated. The inclusion complex was obtained with 71.45% of total recovery and solubility 2.1 times higher compared to the compound in its free form. This increment in solubility was responsible by a tumor growth inhibition potentiation (1.5 times greater compared to compound in its free form). In addition, this study showed that cirsiliol and its inclusion complex in β-cyclodextrin have strong antitumor potential at low doses without promoting side effects commonly observed for conventional drugs as doxorubicin.

1. Introduction

Cancer is one of the major health problems worldwide [1] with an estimation of seven million new cases and 13 million deaths by 2030 according to National Cancer Institute of USA.

Among the cancer therapies, chemotherapy remains one of the most applied to cancer cases. In general, anticancer drugs act not only inhibiting proliferation of tumor cells, but also cell migration, modulating cell metabolism, stimulating the immune response and inducing cell death [2, 3]. However, chemotherapeutic agents have a low selectivity and can affect non-cancer cells, causing several side effects such as myelosuppression, immunosuppression, cardiotoxicity, hepatotoxicity, nephrotoxicity or even general organ toxicity [2, 3, 4, 5]. Other problem associated with chemotherapy is the resistance acquired by several types of cancer [4]. In this sense, the search for new anticancer molecules remains a current approach, privileging compounds capable of maintaining the desired therapeutic effect but without promoting potential toxicity [3, 5].

Historically, natural products have shown to be a promising source for new anticancer molecules. Between 1980-2014 about 1211 new drugs were approved, of which 619 were natural substances or its structures were based on natural products [6, 7]. These compounds exhibit enormous structural diversity, which also provides a diversity of modes of action, including several molecular targets involved.

Among the anticancer molecules extracted from natural sources, we highlight the flavonoid 3′,4′,5-trihydroxy-6,7-dimethoxyflavone, also known as cirsiliol, a natural product found in medicinal plants such as *Leonotis nepetifolia* and others from the Lamiaceae family. This molecule

* Corresponding author.
E-mail address: jackson.guedes@univasf.edu.br (J.R.G.S. Almeida).

https://doi.org/10.1016/j.heliyon.2019.e01692
Received 17 September 2018; Received in revised form 14 April 2019; Accepted 7 May 2019

has sedative, hypnotic, anti-inflammatory properties and selective cytotoxic activity against human tumor cell lines HL-60, SF-295, and OVCAR8 [8, 9, 10, 11].

Although cirsiliol has a potent *in vitro* cytotoxic effect, its aqueous solubility and bioavailability in *in vivo* systems are not satisfactory. To ensure a better profile of solubility, absorption and distribution of natural products with these same characteristics, the use of cyclodextrins has been considered an interesting alternative in recent years. Cyclodextrins are macrocyclic oligosaccharides consisting of (α-1,4)-linked α-*L*-glucopyranose units with a hydrophobic outer surface and hollow hydrophilic interior. Cyclodextrins are able to increase the solubility and bioavailability of molecules poorly soluble in a non-toxic manner through the encapsulating of guest molecule in its hydrophobic internal cavity [12, 13, 14, 15, 16, 17, 18, 19].

Considering the use of cyclodextrins as technological alternative to improve solubility and bioavailability of molecules such as cirsiliol, the present study aimed to obtain an inclusion complex between the carrier β-cyclodextrin and cirsiliol, and to evaluate its cytotoxic potential *in vitro* and antitumor activity *in vivo* compared to the free flavonoid.

2. Materials and methods

2.1. Chemicals and reagents

β-Cyclodextrin was purchased from Cavamax®. MilliQ water was used to prepare the inclusion complex. D_2O was purchased from Tedia® Brasil, MTS aqueous solution ([3-(4,5-dimethylthiazol-2-yl)-5-(3-carboxymethoxyphenyl)-2-(4-sulfophenyl)-2H-tetrazolium, inner salt) was purchased from Promega® and doxorubicin was purchased from Glenmark®.

2.2. Preparation of the inclusion complex

Cirsiliol (6,7-dimethoxy-5,3′,4′-trihydroxyflavone) was previously isolated from the leaves of the species *Leonotis nepetifolia*. Solutions of cirsiliol (CIR) and β-cyclodextrin (CD) in ethanol and water, respectively, were mixed at 1:1 mol proportion in dark glass container and, after 24 h, the organic solvent was evaporated under vacuum. Then, the solution was frozen and dried at -46 °C, 91 × 10^{-3} mBar and the inclusion complex (CD-CIR) stored at 4 °C until further use [16, 20]. The total of recovery was obtained according to the following equation:

$$\text{Total recovery (\%)} = [\text{Recovered powder / Initial (CD + CIR)}] \text{ x } 100$$

To measure the content of CIR in the inclusion complex, the material was suspended in water (50 mL) at room temperature, filtered and after solvent evaporation, the residual mass was measured. The experiment was performed in triplicate and the CIR content in the inclusion complex determined using the following equation:

$$\text{CIR content (\%)} = (\text{Recovered powder / Initial mass of complex}) \text{ x } 100$$

2.3. Preparation of physical mixture (PM-CD-CIR)

Cirsiliol and β-cyclodextrin powders (1:1 molar) were mixed in closed container until a homogeneous mixture be obtained.

2.4. Characterization of the complex of CIR with β-CD

2.4.1. Scanning electron microscopy (SEM)

The surface of materials CD, CIR, (PM-CD-CIR) and CD-CIR were examined by a scanning electronic microscopy (SEM) (Tescan-VEGA3 model). Prior examination, samples were prepared by mounting of powders into carbon tape attached to aluminum stub. The powders were metallized with gold powder for 250 s and then examined using SEM at 10 kV.

2.4.2. Fourier-transform infrared spectroscopy (FTIR) analysis

Further evaluation of complex between cirsiliol and CD was performed by comparisons of CD, CIR, CD-CIR and PM-CD-CIR FTIR spectra. FTIR analyses were performed in a Perkin-Elmer Spectrum, Version 10.4.00 using KBr pellets, scan between 4000 and 650 cm^{-1} and KBr as spectroscopic blank.

2.4.3. Nuclear magnetic resonance (NMR) analysis

1D and 2D ^1H NMR experiments were developed in a Bruker Avance 400 MHz spectrometer. The samples CD and CD-CIR were dissolved in D_2O and the resonance at 4.80 ppm used as internal reference to report chemical shifts values.

2.4.4. Molecular docking analysis

Computational simulations by Molecular Docking were performed to assess, at molecular level, the interaction profile between cirsiliol and CD carrier. Thus, the 3D structure of CD was taken from the RCSB-PDB crystallographic database (www.rcsb.org) (PDB ID: 5MK9). Using the UCSF Chimera package, the complex was edited by removing the co-crystallized protein and adding the hydrogens to the CD. Cirsiliol structure was built on ACD/ChemSketch 12.01 software, followed by a geometry optimization at semi-empirical PM3 level using GaussView 6.0 and Gaussian 09 packages.

The docking algorithm used was the implemented on Autodock v4.2 program and Autodock tools (ADT) v1.5.4 (Autodock, Autogrid, Autotors, Copyright-1991–2000), from the Scripps Research Institute. In this way, Gasteiger charges and polar hydrogens were assigned to CD and CIR. Nonpolar hydrogens were merged. The ligand was considered flexible on analysis and the rotatable bonds were chosen automatically by ADT. The affinity maps were calculated into a grid box containing 30 Å, 30 Å, 30 Å, in order to involve the total structure of CD, with an internal spacing of 0.375 Å between the points. This box was centered on carrier (CD). Lamarckian Genetic Algorithm (LGA) was used to get the most stable conformations of ligand. Initial population was 150, with the maximum number of generations of 27,000. After some tests, the maximum number of energy evaluations was chosen 25,000,000 (long). The default values 0.02 and 0.8 were chosen for mutation and crossover, respectively. The elitism rate was 1.0. In the final docking analysis, was observed the best cluster of conformational similarity, considering binding energy and RMSD (Root Mean Square Deviation) of geometries. The lowest energies conformations of the most populated cluster were considered as the most trustable solutions. The docking profiles were analyzed and discussed in the light of experimental data.

2.4.5. In vitro release studies

Initially, the maximum wavelength for cirsiliol was determined through scanning at wavelengths of 200–400 nm in saline solution (0.15 M) acidified at pH 1.5 with chloride acid, at 37 °C using an Even® UV-Vis spectrophotometer. Further, solutions of cirsiliol range 3.25–26 μg mL^{-1} also to 37 °C were used for build a calibration curve at 215 nm ($Y = 0.0064X + 0.0132$, $R^2 = 0.9959$), where, X is the cirsiliol content and Y absorbance at 215 nm at 37 °C.

For controlled release study, CIR and CD-CIR were placed in 50 mL of saline solution and the experiments was performed at magnetic stirrer with temperature and shaking controlled, 37 °C and 100 rpm, respectively. At periodic intervals, samples of the release medium were taken and analyzed by spectrophotometry at 215 nm to determine the amount of cirsiliol released. All analyses were performed in triplicate for two samples [14, 21].

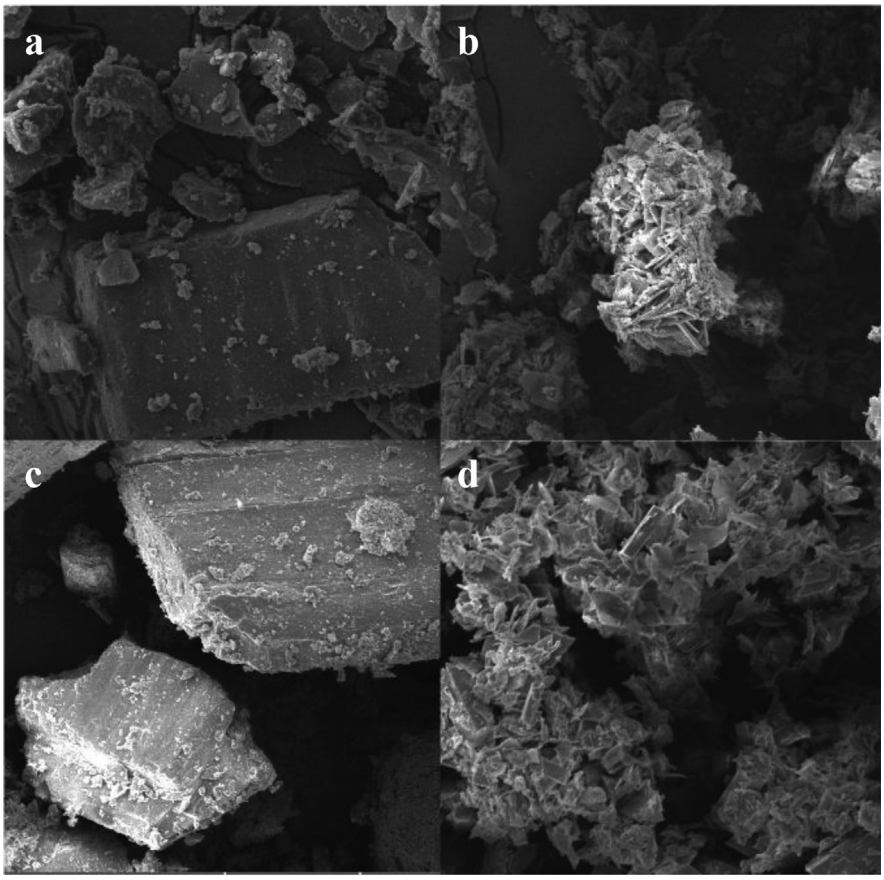

Fig. 1. SEM micrographs: a) beta-cyclodextrin (CD); b) cirsliol (CIR); c) PM-CD-CIR; d) CD-CIR. PM = physical mixture. VEGAN3 TESCAN images with increase 2 K (bar = 20 μm).

2.5. In vitro cytotoxic studies

2.5.1. MTT (3-(4,5-dimethylthiazol-2-yl)-2,5-diphenyltetrazolium bromide) tetrazolium reduction assay

Human prostate cancer (PC3), colon cancer (HCT-116), leukemia (HL-60) and mouse fibroblasts (L929) cell lines ceded by National Cancer Institute of United States were grown in RPMI 1640 medium supplemented with 10% fetal bovine serum and 1% of antibiotics. Cells were maintained at 37 °C in atmosphere with 5% of CO_2.

The cytotoxic assay was performed as described by Skehan et al. (1990) [22]. Briefly, cells were plated in 96-well plate at a density of 0.7×10^5 (HCT-116), 0.3×10^6 (HL-60) and 0.1×10^6 (PC3 and L929) cells per well. Further, cells were treated with several concentrations (10.0–0.31 μg mL^{-1}) of CD-CIR or doxorubicin solubilized in dimethylsulfoxide (DMSO) and allowed to incubation for 72 h. Subsequently, cells were centrifuged and the supernatant was removed. Then, 150 μL of the MTT solution was added and the plates were incubated for 3 h. Absorbance was read after dissolution of the precipitate with 150 μL of pure DMSO in plate spectrophotometer at 595 nm. The IC_{50} was determined for each group through non-linear regression and all experiments performed in triplicate. The selectivity index (SI) was calculated by the ratio of the IC_{50} found for the L929 cells and the IC_{50} found for the tumor cells.

2.5.2. MTS (3-(4,5-dimethylthiazol-2-yl)-5-(3-carboxymethoxyphenyl)-2-(4-sulfophenyl)-2H-tetrazolium) reduction assay

The cytotoxic effect of CIR, CD-CIR inclusion complex, CD and doxorubicin was also evaluated in S-180 murine cell line by MTS reduction assay. Briefly, ascitic fluid was collected from the peritoneal cavity of S-180 mice. A cell suspension was washed with phosphate buffer (PBS, pH 7.4) and centrifuged at 1200 rpm for 3 min. After centrifugation, the supernatant was discarded and the cells were suspended in RPMI 1640 medium supplemented with 10% fetal bovine serum. Tumor cells were counted using trypan blue dye exclusion method, plated in 96-well plate at a density of 1.0×10^5 cell per well and incubated with different concentrations of treatments (1.56–100 μg mL^{-1}) during 24 h at 37 °C [23]. Cell viability was calculated according to the reduction of MTS by mitochondrial enzymes from viable cells, in spectrophotometer at 490 nm, after 3 h of incubation. The IC_{50} was determined for each group through non-linear regression and all experiments were performed in triplicate.

2.6. Animals

Swiss female mice (six weeks old from Federal University of San Francisco Valley) were housed in cages with food and water *ad libitum* and in controlled conditions: 12:12 hour light: dark cycle, 22 ± 3 °C. Animals were treated according to ethical principles of animal experimentation from CEUA (Ethics Committee on the Use of Animals of the Federal University of San Francisco Valley) under protocol number 0002/180716.

2.6.1. In vivo antitumor activity

The *in vivo* antitumor activity was evaluated according to the method described by Chougule et al. (2011) with minimal modifications [4]. The ascitic fluid containing S-180 tumor cells was washed with PBS and centrifuged at 1200 rpm for 3 min. Then, the pellet of cells was suspended in PBS and the number of viable cells was determined using trypan blue dye in Neubauer chamber. After counting, 100 μL of cell suspension (5×10^5 cells) was injected subcutaneously on the back of

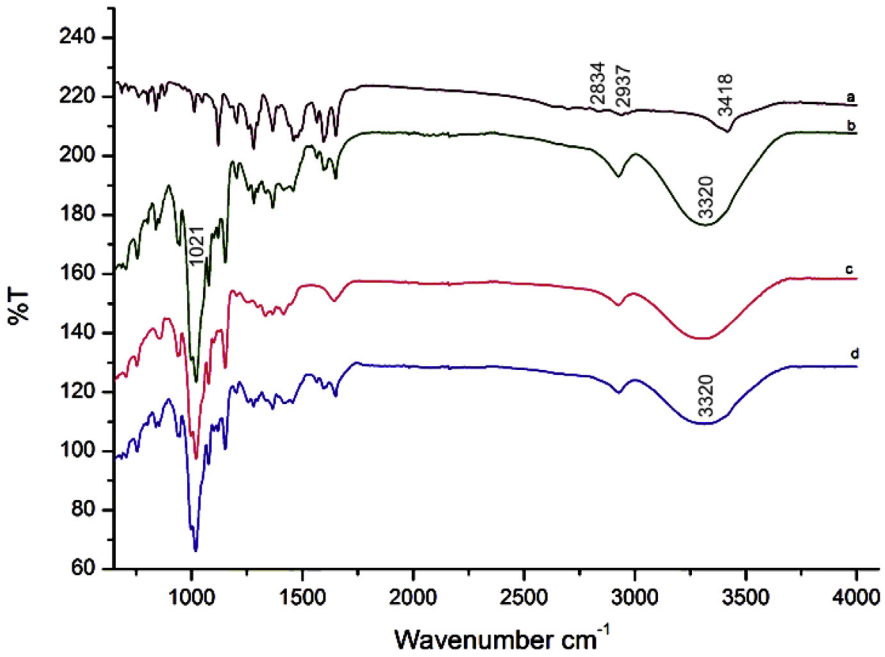

Fig. 2. FTIR spectra a) cirsiliol; b) inclusion complex CD-CIR; c) CD; d) PM-CD-CIR; PM = physical mixture.

each mice. Just animals of SHAM group were not inoculated with S-180 cells.

Animals were distributed in six groups with six animal per cage (n = 6) and treatments started after one week of inoculation. Mice were treated with saline solution (SHAM and negative control), doxorubicin (1.5 mg kg^{-1}), CD-CIR (10 mg kg^{-1}), CIR (10 mg kg^{-1}) and CD (10 mg kg^{-1}). All treatments were performed orally (p.o) once daily for seven days, except doxorubicin treatment (performed intraperitoneally (i.p) in a single dose). Signs of toxicity were verified by monitoring water consumption, feed consumption and body weight once daily throughout the treatment period. On the day 14, mice were euthanized and tumor inhibition ratio (%) was calculated by the follow formula: [(*A-B*)/*A* x 100], where *A* and *B* are the tumor weight average of the negative control, and treated group, respectively [24]. Blood samples were collected from brachial plexus for biochemical and hematological analysis. Tumors, lungs, heart, kidneys, spleen, liver, pancreas, stomach and thymus of each animal were examined according to their anatomy, mass and color changes. Further, portions of tumor, kidneys and liver were prepared with hematoxylin and eosin for histological analysis by light microscopy.

2.7. Statistical analysis

Values are expressed as mean ± S.E.M or mean ± S.D. The differences among experimental groups were compared by ANOVA followed by Tukey ($p < 0.05$) using GraphPad Prism 5.0 software (San Diego, CA).

3. Results and discussion

3.1. Preparation of inclusion complex

Inclusion complexes are often used as alternative to improve solubility, chemical stability, bioavailability and efficiency of poorly soluble compounds such as flavonoids [14, 18, 19, 25], besides decreasing gastric irritation caused by some drugs [13]. To obtain them, several preparation methods can be used, such as coprecipitation, neutralisation, spray drying, freeze-drying, solvent evaporation, ball-milling and sealed-heating [26]. In this study, the freeze-drying method was choice because it is an efficient technique to protect compounds against chemical decomposition, minimize loss of activity due to low processing temperatures, and reduction of the moisture content to very low levels [15]. In cirsiliol-CD inclusion complex, the content of complexed CIR was 17.94 ± 0.48%, the inclusion ratio was 78.00 ± 0.58% and the total recovery was 71.45%. The molecular encapsulation consists in the substitution of water molecules present in the cavity of cyclodextrin by host molecules. This is an energetically favorable processes and stable when occur increase in the entropy and a decrease on system total energy. In this way, the high complexation rate obtained suggests that the material formed is energetically favorable and stable.

3.2. Scanning electron microscopy

As a number of methods can be used to obtain, a range of analytical techniques can be used to ascertain the formation of CD complexes, such as scanning electron microscopy (SEM), infrared spectroscopy (IR), differential scanning calorimetry (DSC), thermogravimetry (TG), ultraviolet spectroscopy (UV-vis), X-ray diffractometry (XRD) and nuclear magnetic resonance spectroscopy (NMR). The combination of informations generated by all these techniques or at least three of these is able to prove whether CD complexes were satisfactorily formed.

The surface morphology of powders materials CD, CIR, PM-CD-CIR, and CD-CIR was obtained by SEM. As shown in Fig. 1, CD presents irregular block structure, whereas CIR presents as agglomerated crystals. In physical mixtures, it was clearly observed the presence of crystalline clusters adhered to the surface of CD, and this image suggests that occurred no interaction between the materials. In contrast, we can observe in CD-CIR inclusion complex the presence of aggregate lamellar films. There is similar profile of lamellar films, as observed by Liu et al. (2017) in inclusion complexes of laccaic acid A in variations of cyclodextrins [19].

3.3. FTIR analysis

In FTIR spectra (Fig. 2), alterations in shift, shape and extinction of peaks were observed, demonstrating a satisfactory inclusion complex formation. Among observed alterations, it is possible to list for guest: disappearance of the peaks at 3418 cm^{-1} (OH axial deformation), 2937 cm^{-1} and 2834 cm^{-1} (CH sp^3, axial deformation), which confirm the inclusion of the guest in host cavity. Further, these results suggest that the

Table 1
Chemical shifts for the protons of CD and CD-CIR inclusion complex.

	δ_{CD}	$\delta_{CD\text{-}CIR}$	$\Delta\delta$
H-1	4.9913	4.9888	-0.0026
H-2	3.5100	3.5096	-0.0004
H-3	3.8892	3.8820	-0.0072
H-4	3.5675	3.5637	-0.0038
H-5	3.7802	3.7687	-0.0115
H-6	3.8006	3.7966	-0,0040

Values express in ppm; *$\Delta\delta = \delta_{CD\text{-}CIR} - \delta_{CD}$; Data obtained from Bruker Avance III 400 MHz. CD = β-cyclodextrin; CD-CIR = inclusion complex (1:1) β-cyclodextrin-cirsiliol.

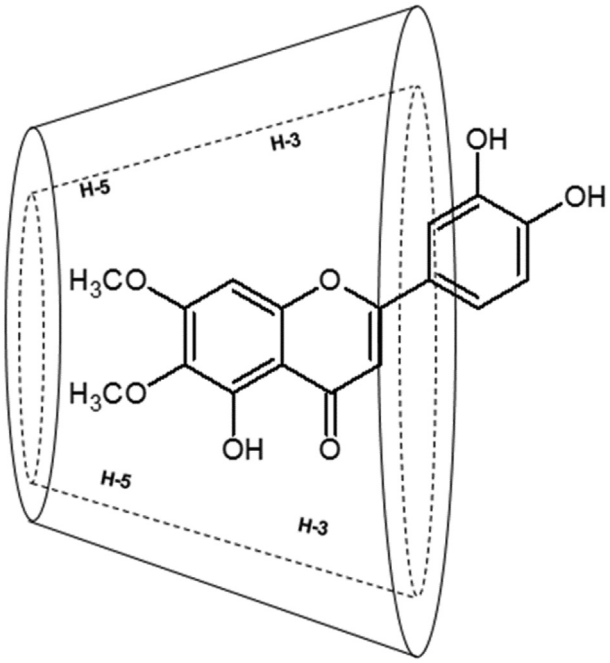

Fig. 3. Possible inclusion mode of cirsiliol in cavity of β-cyclodextrin.

molecule enters in host by means of the condensed rings A and C, portions with the lowest polarity. Others evidences that confirm the inclusion complex formation and the localization of guest in host cavity are the intense shift and increased intensity of band in 3320 cm^{-1} (OH axial deformation of intermolecular bonds). In addition, the maintenance of peak at 1021 cm^{-1} (axial deformation of free OH) suggests no chemical interaction is taking place on the host external face.

3.4. NMR analyses

Proton NMR spectroscopy has been widely used to characterize inclusion complexes involving CDs by comparing the changes in chemical shifts of guest and CDs. Nowadays, NMR is considered the most powerful technique in inclusion complex studies when compared to other techniques such as DSC and FTIR [16, 19]. The NMR spectra of CD, cirsiliol and CD-CIR inclusion complex can be viewed in the Figs. A1–A3, supplementary material). In NMR spectra of CD, data summarized in Table 1, it was observed greater shifts in protons H-3 (0.010 ppm) and H-5 (0.012 ppm). The alterations in these protons, located in host cavity, confirm once more that the guest is in host cavity. Protons H-5 are located inside the cavity, near the narrow side of the cavity and the greater shifts suffered by these protons, allow to affirm that CIR penetrated deeply into CD's cavity by wider side (Fig. 3). The internal cavity of CD have a hydrophobic character and considering that complexation occurs by

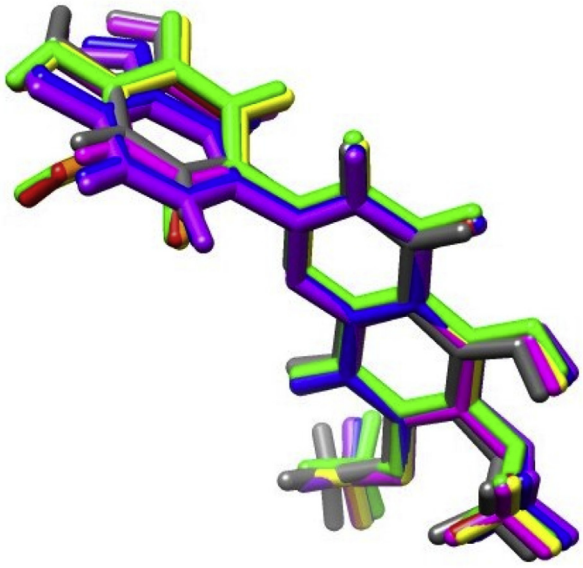

Fig. 4. The eight best conformations of CIR after molecular docking in CD.

molecular interactions, Wan de Walls force for example, it is expected that their internal hydrogens interact with guest non-polar region. Thus, it is expected that the interactions occur among the methoxy groups present in the ring A of cirsiliol and host internal hydrogens. To prove this hypothesis, a ^1H-^1H ROESY spectrum was obtained.

^1H-^1H ROESY NMR experiment is considered one of the most effective techniques to study the internal interactions of host-guest in inclusion complexes. In our complexes, no correlations between hydrogens of two molecules were observed because the resonances of H-3 (3.88 ppm) and H-5 (3.78 ppm) from CD are overlap at resonances of 3.65 ppm (OCH_3-6) and 3.85 ppm (OCH_3-7) from cirsiliol. Thus, to visualize in molecular details the mode of interaction between the guest and host molecules due to gap of ^1H-^1H ROESY information, an *in silico* molecular docking study was developed.

3.5. Molecular docking results

Molecular docking are computational procedures used to simulate, at molecular level, the modes of interactions usually between small ligands and macromolecules, providing an accessible 3D visualization commonly inaccessible by the usual analytical techniques [16]. In this sense, our docking results are in great agreement with analytical evidences, corroborating the possibility of complex formation. Fig. 4 shows the eight best conformations after docking results, demonstrating that cirsiliol has a medium geometric orientation and a preferential occupancy volume within the CD carrier, forming relatively stable complexes. This result demonstrates a conformational profile in the same region, providing reliability to the simulation.

Considering the molecular volume of the flavonoid in the virtual complex generated (Fig. 5), as well other similar studies involving this class of compounds [27, 28] we believe that the host-guest ratio is 1:1. Fig. 5 presents the molecular profile for the best conformation of cirsiliol in the cavity of CD (binding energy = -5.5 Kcal/mol). In the illustration, we can see that the ligand is preferably inserted through the condensed rings. This is noteworthy, since this region does not have free hydroxyls as the opposite phenyl, and the interior of the CD have a nonpolar nature, favoring lipophilic interactions. Our docking results ratify the analysis made for FTIR spectra (extinction of peaks from axial deformation attributed at the methoxyl groups) and ^1H NMR that suggest the interaction of internal hydrogens from host (H-3 and H-5) with guest

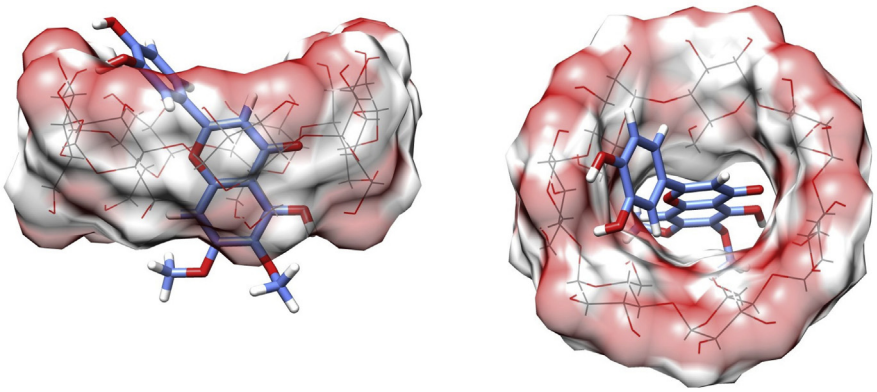

Fig. 5. Best docking conformation for CIR-CD in two visualization modes (the surfaces denote the occupation volume of CD based on Van der Waals radii). CD = β-cyclodextrin; CD-CIR = inclusion complex (1:1) β-cyclodextrin-cirsiliol.

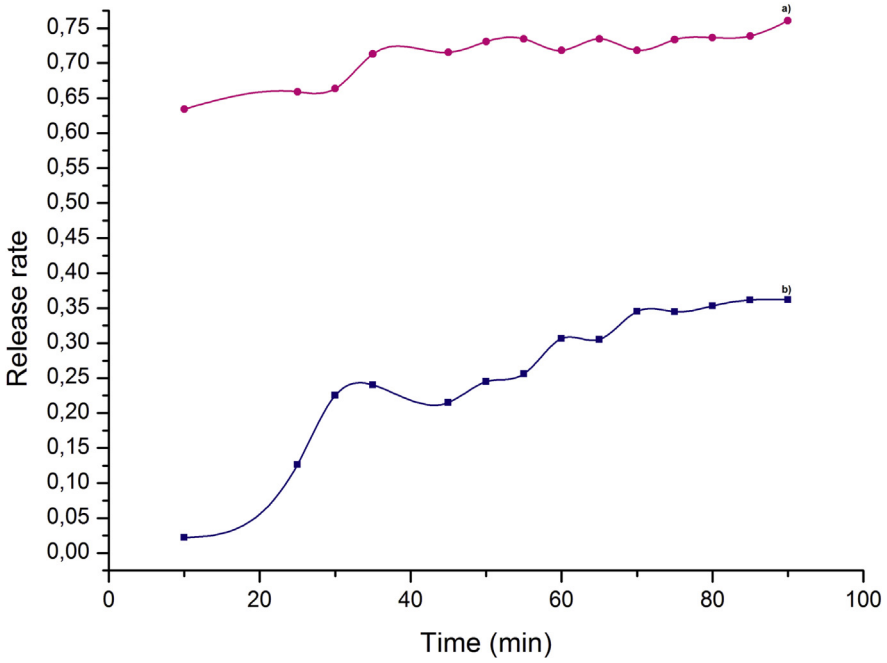

Fig. 6. *In vitro* release study of CD-CIR inclusion complex (a) and CIR (b) in an acidified saline solution (pH 1.5).

molecule.

3.6. In vitro release studies

For pharmaceutical industry, the solubility is a mandatory requirement for the use of molecules as candidates for new drugs, and to achieve this pre-requisite, cyclodextrins are a viable, effective and low toxicity alternative [12, 19, 25].

In vitro release studies using it the vehicle of administration in animals and in conditions similar at the found in stomach (pH 1.5 at 37 °C) is show in Fig. 6. For CD-CIR inclusion complex, the release profile was characterized by a fast release with 63.43% of drug solubilized at first 10 minutes followed by increases in the rate of dissolution reaching 76.1% of the solubilized drug after 90 minutes of analysis. A quite different profile was observed for the CIR. Only 2.2% of the drug has been solubilized in the first 10 minutes and the maximum solubilization at 90 minutes was only 36.2% (Fig. 6). According to Yazan and Sumnu, (1994) the cyclodextrins are able to reduce the solvent surface tension, increasing the solubility of guest and although simple, this study demonstrates the solubility and bioavailability efficiency of proposed formulation. Our inclusion complex increased by 2.1 times the solubilization rate of the molecule under study.

Table 2
IC_{50} values for CD-CIR inclusion complex against human tumor cell lines and against murine normal cell line.

	CD-CIR (IC_{50} $\mu g.mL^{-1}$)	SI	DOXORUBICIN (IC_{50} $\mu g.mL^{-1}$)	SI
HCT-116	5.37	1.30	0.11	9.00
HL-60	3.47	2.01	0.01	99.00
PC3	5.07	1.38	0.44	2.25
L929	6.99	-	0.99	-

Values expressed as media ± standard deviation (n = 2); CD-CIR: inclusion complex (1:1) β-cyclodextrin-cirsiliol; SI (selectivity index).

3.7. In vitro cytotoxic studies

In vitro cytotoxic activity of CD-CIR and positive control doxorubicin were studied against human cancer cell lines HCT-116, HL-60, PC3 and

Table 3
IC_{50} values for CD, CIR, CD-CIR and doxorubicin against S-180 tumor cell line.

CD	CIR	CD-CIR	Doxorubicin
67.06 ± 31.91	7.35 ± 4.87	2.19 ± 1.83	2.53 ± 1.24

Values expressed as media of IC50 ($\mu g.mL^{-1}$) ± standard deviation (n = 3); CD = β-cyclodextrin; CIR = cirsiliol; CD-CIR: inclusion complex (1:1) β-cyclodextrin-cirsiliol.

murine normal cell line (L929). After incubation period, CD-CIR inclusion complex showed strong cytotoxic activity with inhibition of cell growth cellular higher than 75% and values of IC_{50} range among 3.47–5.37 μg mL^{-1} (Table 2) [29]. In this way, CD-CIR can be considered as a drug candidate for cancer therapy.

Although the selectivity index values for positive control doxorubicin have been more expressive that found for CD-CIR inclusion complexes, studies have shown that many tumors have acquired resistant to treatment with this drug. In addition, conventional drugs used in chemotherapy present various side effects as mutagenicity, teratogenicity, nephrotoxicity, neuropathy, myelosuppression, immunosuppression and cardiotoxicity [3, 4, 30]. Thus, the results obtained for the inclusion complex encouraged us to determine the activity against S-180 murine cell line *in vitro* and *in vivo*.

As mentioned before, CDs are extensively used to increase solubility of poorly soluble drugs and many organic compounds. However, in *in vitro* studies this problem can be masked by use of organic solvents as DMSO that increases the solubility of these molecules in samples preparation [18].

To verify the effect of cirsiliol inclusion on the β-cyclodextrin, the cytotoxic activity *in vitro* against the S-180 tumor line cell was performed without solubilize the samples in any organic solvent. The concentrations used for cirsiliol were equivalents to CD-CIR and positive control, ranging from 1.56-100 μg mL^{-1} and IC_{50} was calculated through non-linear regression. As expected, CD-CIR increased the cytotoxic effect of cirsiliol displaying an IC_{50} value of 3.35 μg mL^{-1} (Table 3). This result can be explained by an increase of solubility provided by the CD carrier as verified in the solubility study.

3.8. *In vivo antitumor activity*

In view of the encouraging results of cytotoxic activity *in vitro*, we decided to give continuity to the study by performing the *in vivo* antitumor activity using the S-180 murine line.

After treatment, the animals were sacrificed and the tumors were removed and weighed. The average tumor weight was 0.05 ± 0.04 g in negative control group, while free CIR and CD-CIR inclusion complex were 0.02 ± 0.00 g and 0.01 ± 0.00 g respectively, these results represent 51.34% and 77.03% (*p 0.05*) of reduction in tumor mass, respectively. The group treated with CD-CIR had an inhibition of tumor grown 1.5 higher than group treated with free compound. The pharmacological

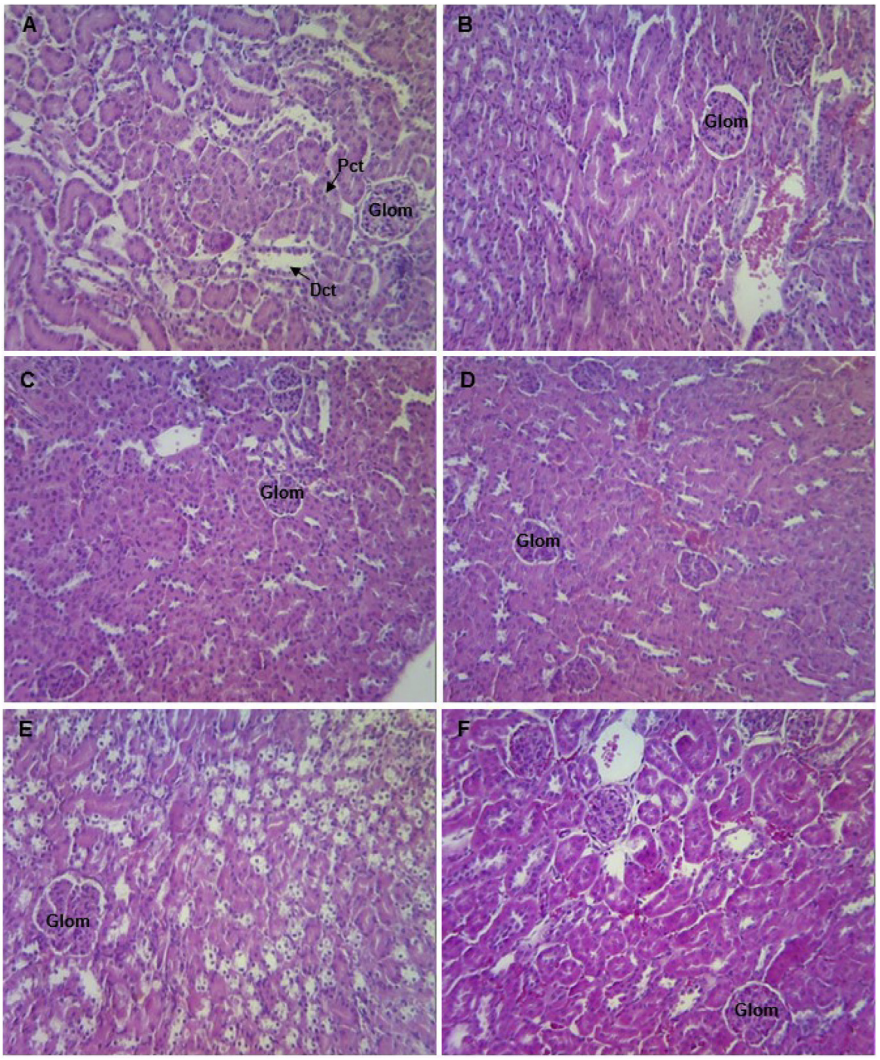

Fig. 7. Histopathological analyses of kidneys removed from healthy control group (panel A); negative control group (panel B); 1.5 mg kg^{-1} doxorubicin-treated group (panel C); 10 mg kg^{-1} cirsiliol-βcyclodextrin-treated group (panel D); 10 mg kg^{-1} cirsiliol-treated group (panel E); and 10 mg kg^{-1} βcyclodextrin-treated group (panel F) analyzed by light microscopy. Histological sections stained with hematoxylin-eosin (100x). Glom: glomerulus, Pct: proximal convoluted tubule, Dct: distal convoluted tubule.

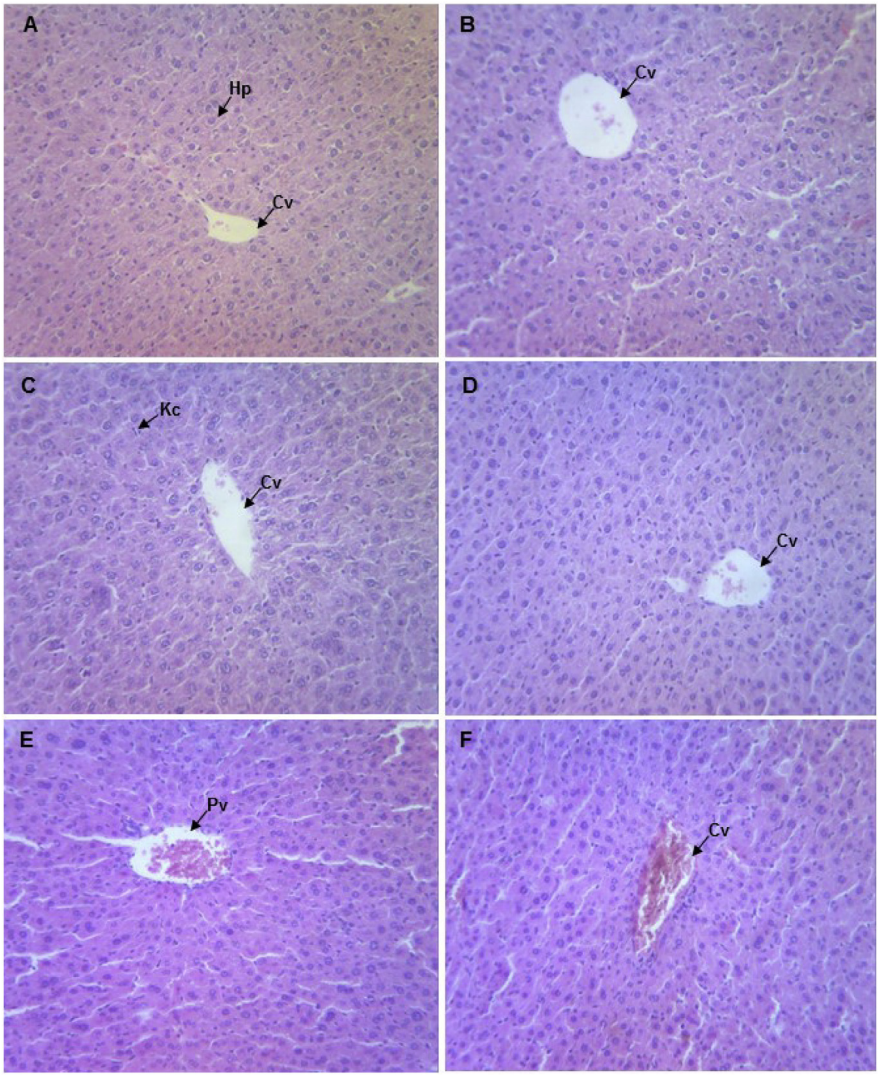

Fig. 8. Histopathological analyses of livers removed from healthy control group (panel A); negative control group (panel B); 1.5 mg kg^{-1} doxorubicin-treated group (panel C); 10 mg kg^{-1} cirsiliol-βcyclodextrin-treated group (panel D); 10 mg kg^{-1} cirsiliol-treated group (panel E); and 10 mg kg^{-1} βcyclodextrin-treated group (panel F), analyzed by light microscopy. Histological sections stained with hematoxylin-eosin (100x). Hp: hepatocyte, Cv: central vein, Pv: portal vein, Kc: kupfer cell.

effects of drugs are directly connected at its solubility and bioavailability. Although not yet well established and controversial about the uptake and bioavailability of flavonoids, some authors claim that the biological potentials exhibited by this class of metabolites have limited activities due to the low rates of absorption and bioavailability. In this way, this fact turns out to be a problem for their application as medicines [31].

The absorption of flavonoids can occur in the small intestine or in the colon after the direct passage through the anterior organ. After absorption, flavonoids undergo biotransformation in the kidneys through the action of enzymes, in the liver by glucuronidation, sulfation and methylation, or can be fragmented into smaller molecules of phenolic compounds. The latter type of biotransformation is also observed in the colon [31, 32].

The release of flavonoids to other tissues and organs occurs only after the biotransformation process is completed. The conjugations suffered tend to decrease the circulation time in plasma as well as facilitate the excretion by the kidneys or colon of the conjugated flavonoids [33]. This decrease in time circulation may still be an additional barrier to the use of flavonoids as medicines. Thus, strategies for increased the time circulation of flavonoids are routinely adopted and the inclusion complexes in cyclodextrins are frequent choices.

As seen in the *in vitro* tests, it is possible to suggest that the greater solubility and bioavailability of compound, promoted by inclusion in CD, are responsible for the increase in the antitumor effect observed (Table A1, Supplementary material). The average tumor weight for doxorubicin was equal to observed for cirsiliol in its free form (0.02 ± 0.01 g), however, two deaths were observed in this group due to its high toxicity.

The possible toxic effects caused by the treatments were also investigated because, in general, antitumor drugs act to prevent the growth or elimination of cancer cells, but this action is extended to healthy cells causing consequently, several side effects [2, 5].

It was observed that the average water consumption of CD-CIR and doxorubicin animals was reduced. Regarding feed intake, no change occurred in CIR or CD-CIR groups, but it was decreased in the doxorubicin group. No alterations in body weight were detected after treatments (Table A2, Supplementary material).

When evaluating the biochemical parameters of the animals (Table A3, Supplementary material), it was observed that the creatinine level in the CD-CIR treated group was high when compared to the SHAM group suggesting a possible nephrotoxicity caused by the formulation [5]. However, evaluation of relative kidney weight (Table A4, Supplementary material) and histopathological analysis showed no change (Fig. 7). Doxorubicin-treated group presented an increase in TGP value

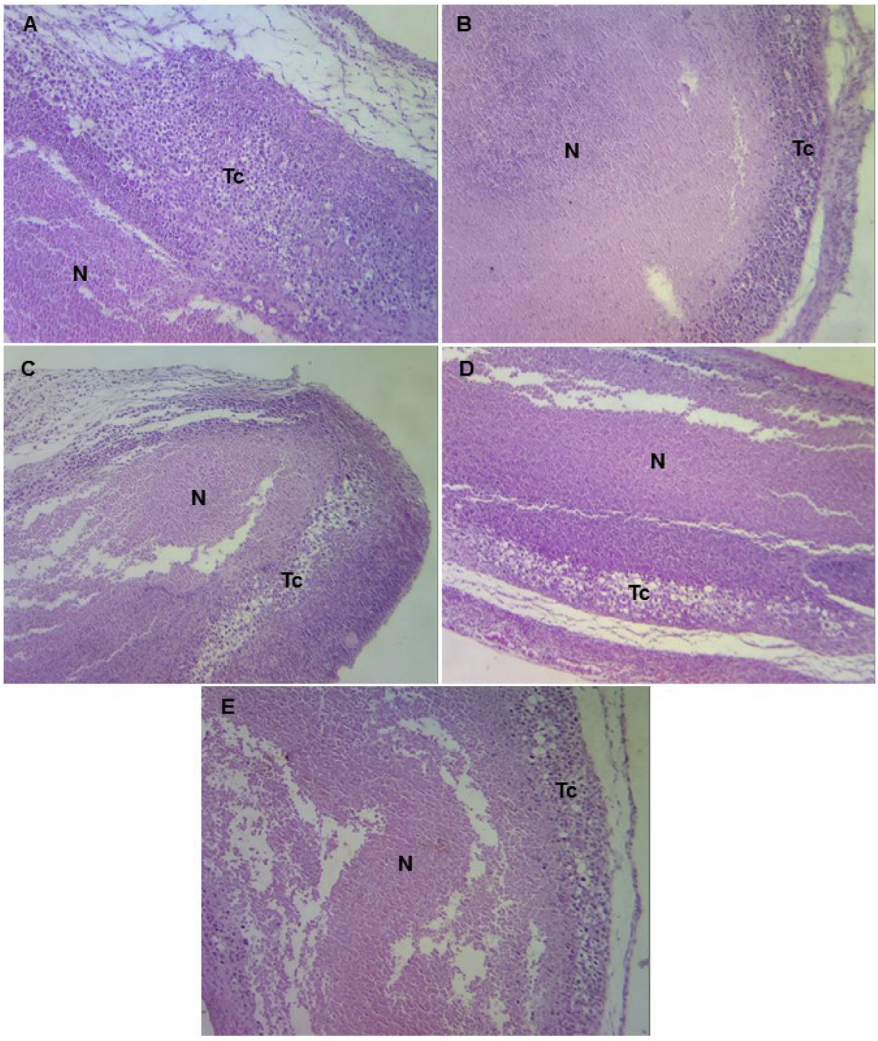

Fig. 9. Histopathological analyses of tumors removed from negative control group (panel A); 1.5 mg kg^{-1} doxorubicin-treated group (panel B); 10 mg kg^{-1} cirsiliol-βcyclodextrin-treated group (panel C); 10 mg kg^{-1} cirsiliol-treated group (panel D); and 10 mg kg^{-1} βcyclodextrin-treated group (panel E) analyzed by light microscopy. Histological sections stained with hematoxylin-eosin (40x).

and in relative liver weight, but no histopathological changes were evidenced (Fig. 8). In addition, in the doxorubicin-treated group the relative weight of the heart was also increased, which reaffirms the side effects reported in literature as cardiotoxicity and hepatotoxicity of this chemotherapy drug [2, 5]. No sign of hematological toxicity was observed after treatment with CIR and CD-CIR (Table A3, Supplementary material).

Finally, the histopathological evaluation of tumors showed solid masses composed of neoplastic polygonal cells with pleomorphic nucleus, mitotic activity, peritumoral inflammatory infiltrate and areas of formation of new capillaries, where these feature varied between groups. Extensive areas of coagulative necrosis were observed in central areas of tumors (Fig. 9). Tumor cells often infiltrated bundles of skeletal striated muscle fibers and lobules of adipose tissue.

4. Conclusions

Our results prove that a stable inclusion complex was obtained between the cirsiliol and the β-cyclodextrin and that the *in vitro* cytotoxic effect against cancer cell lines was maintained or increased by inclusion complex when compared to the results of flavonoid in the free form. The results still showed that the inclusion complex increase the antitumor effect of cirsiliol without associated-side effects observed for the conventional drug (doxorubicin) used in this study.

Declarations

Author contribution statement

Ana P. Oliveira, Andressa L.N. Silva, Lucas G.F.C. Viana, Mariana G. Silva, Érica M. Lavor, Raimundo G. Oliveira-Júnior, Edilson B. Alencar-Filho, Ricardo S. Lima, Rosemairy L. Mendes, Larissa A. Rolim, Débora S.C. Anjos, Leslie R.M. Ferraz, Pedro J. Rolim-Neto, Maria F.S. Silva, Claudia do Ó Pessoa, Jackson R.G.S. Almeida: Conceived and designed the experiments; Performed the experiments; Analyzed and interpreted the data; Contributed reagents, materials, analysis tools or data; Wrote the paper.

Funding statement

This research did not receive any specific grant from funding agencies in the public, commercial, or not-for-profit sectors.

Competing interest statement

The authors declare no conflict of interest.

Additional information

Supplementary content related to this article has been published online at https://doi.org/10.1016/j.heliyon.2019.e01692.

References

[1] A. Subastri, V. Arun, P. Sharma, E.P. Babu, A. Suyavaran, S. Nithananthan, G.,M. Alshammari, B. Aristatile, V. Dharuman, C. Thirunavukkarasu, Synthesis and characterisation of arsenic nanoparticles and its interaction with DNA and cytotoxic potential on breast cancer cells, Chem. Biol. Interact. (2017) 1–11.

[2] H.I. El-Sayyad, M.F. Ismail, F.M. Shalaby, R.F. Abou-El-Magd, R.L. Gaur, A. Fernando, M.H.G. Raj, A. Ouhtit, Histopatological effects of cisplatin, doxorubicin and 5-fluoracil (5-FU) on the liver of male albino rats, Int. J. Biol. Sci. 5 (2009) 466–473.

[3] P. Rathee, D. Rathee, D. Rathee, S. Rathee, In-vitro cytotoxic activity of β-sitosterol triacontane isolated from *Capparis decidua* (Forsk.) Edgew, Asian J. Pac. Trop. Med (2012) 225–230.

[4] M.B. Chougule, A.R. Patel, T. Jackson, M. Singh, Antitumor activity of noscapine in combination with doxorubicin in triple negative breast cancer, PLoS One 6 (2011) 1–12.

[5] L.N. Andrade, R.G. Amaral, G.A.A. Dória, C.S. Fonseca, T.K.M. Silva, R.L.C. Albuquerque Jr., S.M. Thomazzi, L.G. Nascimento, A.A. Carvalho, D.P. Sousa, In Vivo anti-tumor activity and toxicological evaluations of perillaldehyde 8,9-epoxide, a derivative of perillyl alcohol, Int. J. Mol. Sci. 17 (2016) 1–11.

[6] T.J. Makhafola, E.E. Elgorashi, L.J. McGaw, L. Verschaeve, J.N. Eloff, The correlation between antimutagenic activity and total phenolic content of extracts of 31 plant species with high antioxidant activity, BMC Complement Altern. Med. 16 (2016) 490–503.

[7] D.J. Newman, G.M. Cragg, Natural products as sources of new drugs from 1981 to 2014, J. Nat. Prod. 79 (2016) 629–661.

[8] H. Viola, C. Wasowski, M. Marder, C. Wolfman, A.C. Paladini, J.H. Medina, Sedative and hypnotic properties of *Salvia guaranitica* St. Hll. and of its active principle, Cirsiliol, Phytomedicine 4 (1997) 47–51.

[9] N. Bai, H. He, Z. Zhou, C. Lai, L. Zhang, Z. Quan, X. Shao, M. Pan, C. Ho, Flavonoids from *Rabdosi arubescens* exert anti-inflammatory and growth inhibitory effect against human leukemia HL-60 cells, Food Chem. 122 (2010) 831–835.

[10] J. Li, F.R. Fronczec, D. Ferreira, C.L. Burandt Jr., V. Setola, B.L. Roth, J.K. Zjawiony, Bis-spirolabdane diterpenoids from *Leonotis nepetaefolia*, J. Nat. Prod. 75 (2012) 728–734.

[11] A.P. Oliveira, A.L. Guimarães, A.M. Pacheco, C.S. Araújo, R.G. Oliveira Jr., E.M. Lavor, M.G. Silva, E.C.C. Araújo, R.L. Mendes, L.A. Rolim, M.P. Costa, H.C.L. Farias, C.O. Pessoa, N.P. Lopes, L.M.M. Marques, J.R.G.S. Almeida, Estudo fitoquímico, atividade antimicrobiana e citotóxica de espécimes de *Leonotis nepetifolia* L. R. (Br), Quim. Nova 1 (2016) 32–37.

[12] T. Loftsson, D. Hreinsdóttir, M. Másson, Evaluation of cyclodextrin solubilization of drugs, Int. J. Pharm. 302 (2005) 18–28.

[13] F.L. Guedes, G.M.C. Alves, F.L.A. Santos, L.F. Lima, L.A. Rolim, P.J.R. Neto, Ciclodextrinas: como adjuvante tecnológico para melhorar a biodisponibilidade de fármacos, Rev. Bras. Farm. 89 (2008) 220–225.

[14] J. Wang, Y. Cao, B. Sun, C. Wang, Physicochemical and release characterisation of garlic oil-β-cyclodextrin inclusion complexes, Food Chem. 127 (2011) 1680–1685.

[15] J. Wang, Y. Cao, B. Sun, C. Wang, Characterisation of inclusion complex of trans-ferulic acid and hydroxypropyl-β-cyclodextrin, Food Chem. 124 (2011) 1069–1075.

[16] V. Jahed, A. Zarrabi, A. Bordbar, M.S. Hafezi, NMR (^{1}H, ROESY) spectroscopic and molecular modelling investigations of supramolecular complex of β-cyclodextrin and curcumin, Food Chem. 165 (2014) 241–246.

[17] C. Yuan, Z. Lu, Z. Jin, Characterization of an inclusion complex of ethyl benzoate with hydroxypropryl-β-cyclodextrin, Food Chem. 152 (2014) 140–145.

[18] M. Poorghorban, U. Das, O. Alidi, J.M. Chitanda, D. Michel, J. Dimmock, R. Verrall, P. Grochulski, I. Badea, Characterization of the host-guest complex of a curcumin analog with β-cyclodextrin and β-cyclodextrin-gemini surfactant and evaluation of its anticancer activity, Int. J. Nanomed. 10 (2015) 503–515.

[19] L. Liu, J. Xu, H. Zheng, K. Li, W. Zhang, K. Li, H. Zhang, Inclusion complexes of laccaic acid A with β-cyclodextrin or its derivatives: phase solubility, solubilization, inclusion mode, and characterization, Dyes Pigments 139 (2017) 737–746.

[20] L.F. Fraceto, M.M. Gonçalves, C.M. Moraes, D.R. Araújo, L. Zanella, E. Paula, T.A. Pertinhez, Caracterização do complexo de inclusão ropivacaína:β-ciclodextrina, Quim. Nova 30 (2007) 1203–1207.

[21] Y.M.S. Pires, L.R. Almeida, L.M.A. Meirelles, Perfil de dissolução do tenoxicam em complexos de inclusão de beta-ciclodextrinas, Eletronic J. Pharm. 13 (2016) 64–70.

[22] P. Skehan, R. Storeng, D. Scudiero, A. Monks, J. McMahon, D. Vistica, J.T. Warren, H. Bodesch, S. Kenney, M.R. Boyd, New colorimetric cytotoxicity assay for anticancer – drug screening, J. Natl. Cancer Inst. 82 (1990) 1107–1112.

[23] PITA, João Carlos Lima Rodrigues, Avaliação da atividade antitumoral e citotoxicidade do Trachylobano-360 de Xylopia langsdorffianna St. Hil.&Tul. (Annonaceae). 2010. 105f: Dissertação de mestrado (Programa de pós-graduação em Produtos Naturais e Sintéticos Bioativos), Universidade Federal da Paraíba, Paraíba, 2010.

[24] R.C. Montenegro, R.A.F. Farias, M.R.P. Pereira, A.P.N.N. Alves, F.S. Bezerra, M. Andrade-Neto, C. Pessoa, M.O. Moraes, L.V. Costa-Lotufo, Antitumor activity of pisosterol in mice bearing with S180 tumor, Bio. Pharm. Bull. 31 (2008) 454–457.

[25] S.S. Jambhekar, P. Breen, Cyclodextrins in pharmaceutical formulations II: solubilization, binding constant, and complexation efficiency, Drug Discov. Today 21 (2016) 363–368.

[26] T. Yamada, T. Imai, k. Ouchi, M. Otagiri, F. Hirayama, K. Uekama, Inclusion complex of 3,9-bis(N,N-dimethylcarbamoyloxy)-5H-benzofuro[3,2-c]quinoline-6-one (KCA-098) with Heptakis(2,6-di-*O*-methyl)-β-cyclodextrin: interaction and dissolution properties, Chem. Pharm. Bull. 48 (2000) 1264–1269.

[27] L.J. Yang, S. Xia, S.X. Ma, S.Y. Zhou, X.Q. Zhao, S.H. Wang, M.Y. Li, X.D. Yang, Host-guest system of hesperetin and β-cyclodextrin or its derivatives: preparation, characterization, inclusion mode, solubilization and stability, Mater. Sci. Eng. C 59 (2016) 1016–1024.

[28] R. Zha, C. Sandström, H. Zhang, T. Tan, NMR study on the inclusion complexes of β-cyclodextrin with Isoflavones, Molecules 21 (2016) 372–382.

[29] B.S.F. Rodrigues, B.D.B. Sahm, P.C. Jimenez, F.C.L. Pinto, J. Mafezoli, M.M. Mattos, E. Rodrigues-Filho, L.H. Pfenning, L.M. Abreu, L.M. Abreu, L.V. Costa-Lotufo, M.C.F. Oliveira, Bioprospection of cytotoxic compounds in fungal strains recovered from sediments of Brazilian coast, Chem. Biodivers. 12 (2015) 432–442.

[30] D. Wang, S. Peng, A.R.M.R. Amin, M.A. Rahman, S. Nannapaneni, Y. Liu, D.M. Shin, N.F. Saba, J.F. Eichler, Z.G. Chen, Antitumor activity of 2,9-di-sec-butyl-1,10-phenathroline, PloS One 11 (2016) 1–14.

[31] S. Kumar, A.K. Pandey, Chemistry and biological activities of flavonoids: an overview, Sci. World J. 2013 (2013) 1–16.

[32] P.C.H. Hollman, Absorption, bioavailability, and metabolism of flavonoids, Pharmaceut. Biol. 42 (2004) 74–83.

[33] M. Akhlaghi, Sahar. Foshati, Bioavailability and metabolism of flavonoids: a review, Int. J. Nutr. Sci. 2 (2017) 180–184.